International Journal of Mass Spectrometry 303 (2011) 125–128

Contents lists available at ScienceDirect

International Journal of Mass Spectrometry

journal homepage: www.elsevier.com/locate/ijms

Dissociative electron attachment to carbonyl fluoride, F_2CO

M. Hoshino [a,**], P. Limão-Vieira [a,b,*], M. Probst [c], Y. Nunes [b], H. Tanaka [a]

[a] Department of Material and Life Sciences, Sophia University, Chiyoda-ku, Tokyo 102-8554, Japan
[b] Laboratório de Colisões Atómicas e Moleculares, CEFITEC, Departamento de Física, FCT, Universidade Nova de Lisboa, 2829-516 Caparica, Portugal
[c] Institut für Ionenphysik and Angewandte Physik, Universität Innsbruck, Technikerstraβe 25, A-6020 Innsbruck, Austria

ARTICLE INFO

Article history:
Received 21 September 2010
Received in revised form 17 January 2011
Accepted 17 January 2011
Available online 21 February 2011

Keywords:
Carbonyl fluoride
Negative ions
Mass spectrometry
Quantum chemical calculations

ABSTRACT

Low energy electron attachment to gas phase carbonyl fluoride, F_2CO, has been performed by means of a crossed electron-molecular beam experiment in an electron energy range from 0 to 30 eV with an energy resolution of ~0.5 eV. The most intense signal is observed at 19 amu due to F^- and two other anionic species with lower intensities at 38 and 47 amu assigned to F_2^- and COF^-, respectively. Anion efficiency curves of the three anions have been measured. Product anions (F^- and COF^-) are observed mainly in the low energy region arising from simple bond breaking, while F_2^- is being produced from two bond cleavages with further structural and electronic rearrangement. Quantum chemical calculations on the electronic properties of F_2CO have been performed in order to complement the experimental results.

© 2011 Elsevier B.V. All rights reserved.

1. Introduction

Further to the global effort in reducing emissions under the Kyoto protocol, carbonyl fluoride, F_2CO, has been suggested as a suitable candidate for replacement feed gas to the traditional highly global warming SF_6 and other perfluorocarbons used in the plasma semiconductor industry. F_2CO has been extensively used as a cleaning agent in chemical vapour deposition equipment, as well.

Carbonyl fluoride has been the subject of a few experimental studies on photoelectron [1–3] and VUV photoabsorption [4] spectroscopies while the only published electron impact vibrational excitation result is the relatively high resolution data of Kato et al. [5]. Recently we have reported on the first complete Electron Energy Loss Spectroscopy (EELS) data of carbonyl fluoride from 5.0 to 18.0 eV [6]. Meanwhile theoretical studies of the ultraviolet (UV) and photoelectron spectrum of carbonyl fluoride by multireference configuration interaction methods have been reported [7] and molecular-adapted quantum defect orbital (MQDO) procedures used for calculating the spectral intensities of Rydberg transitions.

Brundle et al. [1] studies on the photoelectron spectra of hydrocarbons with fluorine substitution have shown that ionisation from π orbitals are not affected under substitution, but shifted from σ orbitals to higher energies. This σ orbital stabilisation is known as the perfluoro-effect and is observed clearly in the comparison of the photoelectron spectra of F_2CO and H_2CO.

As far as we are aware no dissociative electron attachment studies to carbonyl fluoride have been reported. In the present work we investigate the negative ion formation from F_2CO at low electron energies (0–30 eV) by recording the ion yield curves with an electron energy resolution of ~500 meV. No parent anion has been observed. The by far dominant signal can be assigned to F^- formation. It is shown that three DEA products are formed at electron energies near 2–3 eV (Table 1).

2. Experimental and computational details

Electron attachment to F_2CO was investigated by using a tuneable electron source assembled directly at the entrance of a quadrupole mass spectrometer (QMS) (Hiden Analytical Ltd. HAL 301 s/2). Briefly, a ~500 meV (FWHM), electron beam is produced in a commercial electron gun with typical currents of ~500 nA that crosses the effusive molecular beam emerging through a capillary. Negative ions formed in the interaction region are extracted by weak electric fields (3.0 V), focused by a set of einzel lens, mass analyzed by means of a quadrupole mass filter and detected in a channel electron multiplier operated in pulse counting mode. The electron energy scale as well as the electron energy resolution is calibrated using the well known negative ion yields of O^- from CO, near 9.5 eV [8], and from CO_2, near 4.4 and 8.1 eV [9].

The time span from ion formation to its detection is in the order of microseconds. Negative ion yields are obtained as a function of

---

* Corresponding author at: Laboratório de Colisões Atómicas e Moleculares, CEFITEC, Departamento de Física, FCT, Universidade Nova de Lisboa, 2829-516 Caparica, Portugal. Tel.: +351 21 294 85 76; fax: +351 21 294 85 49.
** Co-Corresponding author at: Department of Physics, Sophia University. Tel.: +81 3 3238 4227; fax: +81 3 3238 3341.
E-mail addresses: masami-h@sophia.ac.jp (M. Hoshino), plimaovieira@fct.unl.pt (P. Limão-Vieira).

1387-3806/$ – see front matter © 2011 Elsevier B.V. All rights reserved.
doi:10.1016/j.ijms.2011.01.013

Table 1
Peak positions for the fragment anions of F_2CO.

Mass (dalton)	Anionic species assignment	Peak position in eV[a]	
47	COF^-	2.00	2.62
38	$F_2{}^-$	–	2.40
19	F^-	0.75	2.15

[a] Value obtained through Gaussian fitting profiles.

Table 2
Calculated geometry of carbonyl fluoride with bond lengths in Å and angles in (°).

	Anion		Ground state B3LYP/aug-cc-pVTZ
	C_{2v}	C_S	C_{2v}
C–O	1.225	1.219	1.171
C–F	1.371	1.470	1.319
∠F–C–O	126.38	117.18	126.16
∠F–C–F	–	108.00	–

the electron energy. The typical base pressure in the main chamber was 2.0×10^{-5} Pa and upon gas admission (F_2CO) increased to a pressure of 1.3×10^{-4} Pa. The gas sample was supplied from Daikin Co. and used as delivered. The stated purity was 99.9%.

To complement the experimental results, we carried out quantum chemical calculations on the electronic properties of F_2CO. We optimized the molecular geometries of F_2CO by using the B3LYP [10] density functional and the aug-cc-pVTZ basis set [11]. On this level of theory F_2CO has a dipole moment of 1.03 Debye. This value is close to that reported from a microwave experiment (0.91) [12] and also from MP2 calculations (0.95) [13]. Moreover the calculated geometrical parameters (Table 2; $r_{CF} = 1.319$, $r_{CO} = 1.171$, $\angle_{FCF} = 108°$) differ only insignificantly from the experimentally derived values ($r_{CF} = 1.312$, $r_{CO} = 1.174$, $\angle_{FCF} = 108°$) [11]. While the ground state of F_2CO is planar with C_{2v} symmetry, the equilibrium conformation of the anion is C_s-pyramidal. The transient negative ion (TNI) formed by vertical electron attachment to the equilibrium geometry of the neutral molecule is thermodynamically unstable. However, the adiabatic electron attachment is slightly exothermic and the anion in the optimal pyramidal structure has a small positive electron affinity of 0.21 eV. Outer-valence Greens' function calculations [14] were used to model the vertical electron attachment to the LUMO of the neutral molecule.

3. Results and discussion

Fig. 1 shows the electron energy dependence of the ion yield for the three negative ions of F_2CO measured with an electron energy resolution of ∼500 meV (FWHM). The most dominant fragment anion is F^- (19 amu), followed by $F_2{}^-$ (38 amu) and COF^- (47 amu). The negative ion resonances have been fitted with Gaussian profile curves in order to resolve the features to obtain the maximum values (Table 1). The present electron energy resolution of ∼500 meV (FWHM) can explain the absence of a parent anion signal. However autodetachment or fragmentation in a time window shorter than the experimental detection times may also be responsible for the lack of such anion. The considerable change in geometry from the neutral to the anion might explain the instability of the F_2CO with respect to autodetachment and furthermore, the localization of the extra charge over the fluorine atoms (Fig. 2(b)) may result in rapid fragmentation of the parent negative ion.

Fig. 2(a and b) shows the optimized geometries from aug-cc-pvTZ calculations for the ground state of the neutral and the negative ion, respectively, along with their highest occupied molecular orbitals (HOMOs). The geometry of the negative ion reveals noticeable changes in respect to the neutral. The HOMO in F_2CO^- also reveals the excess electron localized in the fluorines with nodes along the C–F bonds. Fig. 2(c) shows the lowest unoccupied molecular orbital (LUMO). The vertical attachment energy of F_2CO calculated by the OVGV method is 1.21 eV.

3.1. Ion yield curves

Capture of a free electron by a polyatomic neutral molecule, ABC, yields negative ion formation generating a transient negative ion (TNI), $(ABC)^{\#-}$, that may decompose into either reaction (1a) $AB + C^-$ or (1b) $AC + B^-$. The TNI is seen as a quasi-bound state embedded in the autodetachment continuum and is therefore unstable towards the loss of the extra charge. The autodetachment lifetime varies, depending on the nature of the target molecule and on the electron energy, from a few fs as is the case of $N_2{}^-$ [15] and up to several tens of μs for $C_{60}{}^-$ [16]. F_2CO is a polyatomic molecule that belongs to a group where autodetachment may occur in a time window shorter than the detection time, resulting in the absence of

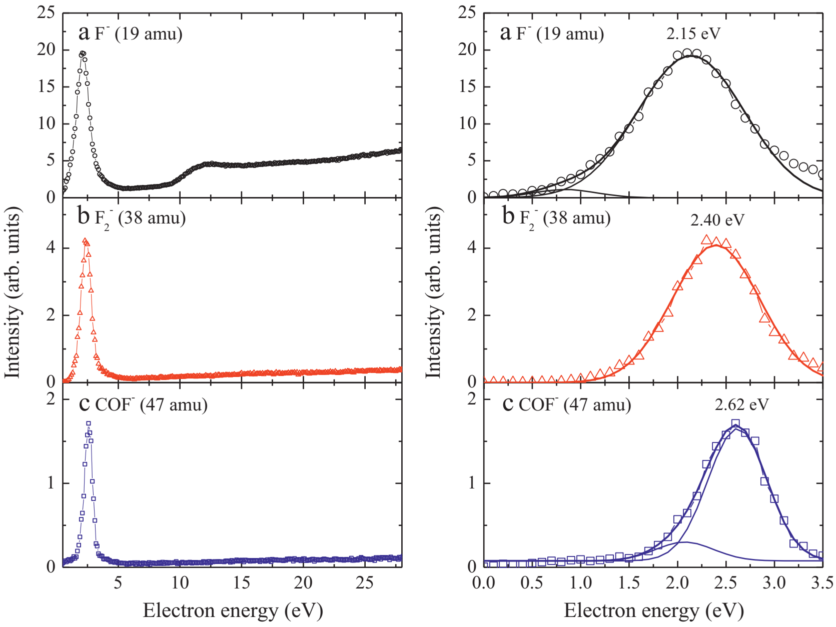

Fig. 1. Anion efficiency curves of the three product anions formed by DEA to F_2CO.

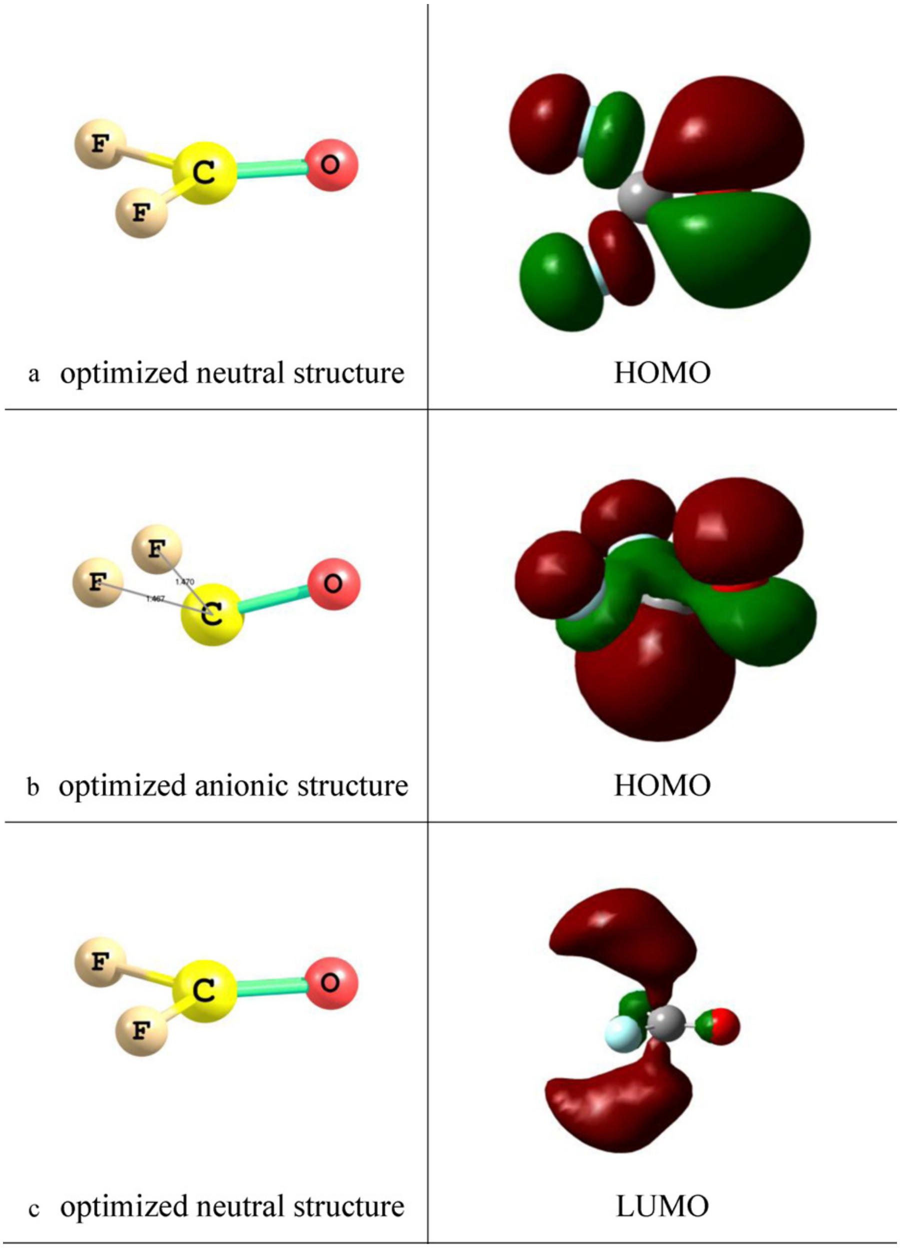

Fig. 2. Optimized structures of F_2CO as neutral (a) and negatively charged (b) molecule. The highest occupied molecular orbital of the neutral molecule (a) and of the anion (b) and the lowest unoccupied molecular orbital of the neutral (c) are shown as isosurfaces. All results were obtained at the B3LYP/aug-cc-pVTZ level of theory.

an observable parent anion. That tendency is also increased by the considerable change in geometry from the neutral to the anion, resulting in the delocalization of the extra charge over the C–F groups (Fig. 2), leading to fragmentation. In addition Table 1 gives the corresponding peak's positions of the resonances. The TNIs generated at low energy may be assigned as shape resonances involving the π^* antibonding orbitals.

For DEA channels energetically accessible from the TNI, decomposition can take place prior to the loss of the extra electron. The threshold energy (E_{th}) determined by energy conservation of the DEA reaction

$$e^- + ABC \rightarrow (ABC)^{\#-} \rightarrow AB + C^- \tag{1a}$$

$$e^- + ABC \rightarrow (ABC)^{\#-} \rightarrow AC + B^- \tag{1b}$$

is given by:

$$E_{th} = D(AB - C) - EA(C) + E* \tag{2a}$$

with D(AB–C) the binding enthalpy of the chemical bond, EA(C) the electron affinity of the (neutral) fragment carrying the extra charge and E^* the total excess energy. Though, as far as standard heats of formation (ΔH_f^o) are concerned, Eq. (2a) can be written as:

$$E_{th} = \Delta H_R^o = \Delta H_f^o(AB) + \Delta H_f^o(C^-) - \Delta H_f^o(ABC) \tag{2b}$$

where ΔH_R^o represents the standard heat of reaction (1a) with $\Delta H_f^o(C^-) = \Delta H_f^o(C) - EA(C)$. The threshold energy for reaction (1a) is typically below 4 eV [17], for the case that the anion is formed by simple bond-cleavages and no rearrangement processes in a neutral fragment take place. This is due to the fact that the electron affinity for most radicals is usually less than 4 eV below the bond dissociation energy. However, for more complicated reactions involving rearrangement, as is depicted in reaction (1b), the energy gain by formation of the highly stable neutral products AC can shift the threshold energy to very low values [18].

Table 3
Gas phase standard heats of formation (ΔH_f^o) and electron affinities relevant in dissociative electron attachment to F_2CO (obtained from Ref. [19]).

Compound	ΔH_f^o (eV)
F_2CO	−6.62
COF	−1.78
CO	−1.15
F	0.82
COF^-	–
F_2^-	-3.02 ± 0.07
F^-	–
	Electron affinity (eV)
F_2CO	–
COF	3.3
F_2	3.120 ± 0.070
CO	1.3261
F	3.4012

3.2. *The complementary ions F^- (19 amu) and COF^- (47 amu)*

These ions are formed via the cleavage of one of the C–F bonds leading to the complementary DEA reactions with respect to the extra charge:

$$e^- + F_2CO \rightarrow (F_2CO)^{\#-} \rightarrow [COF] + F^- \tag{3a}$$

$$e^- + F_2CO \rightarrow (F_2CO)^{\#-} \rightarrow [COF] + F \tag{3b}$$

Fig. 1 upper and lower panels show the ion yield curve for F^- and COF^-, respectively. Reaction (3a) is endothermic by 2.26 eV as derived from the bond dissociation energy D(C–F) = 5.66 eV (difference between the standard heat of formation for F_2CO and the sum of the standard heats of formation for FCO and F) and the well known electron affinity EA(F) = 3.4 eV [19], while reaction (3b) is also endothermic by 2.36 eV, taking the EA([COF]) = 3.3 eV [19]. The experimental appearance energies of F^- and COF^- ions (Fig. 1) are below the calculated threshold. However one should not discard the possibility that decomposition of F_2CO at the hot filament surface or any impurities may contribute as a possible source for the pre-threshold contribution in the F^- and COF^- ion yields. With the thermochemical data of Table 3 for the reactions (3a) and (3b), the $\Delta H_f^o(F^-) = -2.58$ eV and $\Delta H_f^o(COF^-) = -5.08$ eV, respectively, when the reactions proceed without excess energy (at the appearance energy).

The main resonances around 2.2–2.6 eV (Table 1) have been assigned to shape resonances, which may decompose via one anion fragment plus one neutral. The F^- and COF^- ionic yields increase above 10 and 15–16 eV (Fig. 1), respectively, suggesting ion pair formation. Taking into account the AE(COF^+) = 11.26 eV and AE(F^+) = 17.42 eV [19], and bearing in mind the present rather low energy resolution (~500 meV) such an assumption seems reasonable.

3.3. *F_2^- (38 amu)*

Formation of F_2^- (Eq. (4)) requires:

$$e^- + F_2CO \rightarrow (F_2CO)^{\#-} \rightarrow [CO] + F_2^- \tag{4}$$

Formation of F_2^- requires the cleavage of two C–F bonds and the formation of an F–F bond to yield the stable fragments. Taking the thermochemical data from Table 3, reaction (4) is endothermic by 2.46 eV. Taking the electron affinity of 3.12 eV and a threshold of ~1.5 eV in Fig. 1, we get an estimate for the dissociation energy of 1.62 eV. It is interesting to note that in condensed phase studies on fluorinated compounds like SF_5CF_3, the molecular ion F_2^- is also observed but at somewhat higher electron energies. This ion was not detected in DEA from gas phase and was proposed to be a product of a secondary reaction like F^- formation via DEA and reactive scattering with neighbouring molecules creating F_2^- [20]. In contrast, in the present gas phase system the LUMO wave function (Fig. 2(c)) shows an extended profile from the carbon site to the fluorines. The mechanism yielding F_2^- formation proceeds through the attachment of the extra electron and two C–F bond ruptures. Such configuration may imply considerable geometry change in the temporary negative ion (Fig. 2), which is supported by the calculations shown in Table 2.

4. Conclusions

The present DEA study on F_2CO shows the ionic yields measured in the electron energy range of 0–30 eV with a tuneable electron source assembled directly to the entrance of a quadrupole mass spectrometer. Capture of low energy electrons at around 2.0 eV by F_2CO shows the formation of fragments with the most dominant DEA reaction leading to F^- (19 amu). In addition, production of COF^- (47 amu) and F_2^- (38 amu) has also been observed.

Acknowledgments

PL-V acknowledges his Visiting Professor position at Sophia University, Tokyo, Japan. This work is performed with the support and under the auspices of the NIFS Collaboration Research program (NIFS08KYAM017). This work also forms part of the EU COST Actions CM0601 and CM0805 programmes “ECCL” and “The Chemical Cosmos”, respectively. MP acknowledges support from the RFBR-FWF projects 09-03-91001-a and I200-N19.

References

[1] C.R. Brundle, M.B. Robin, N.A. Kuebler, H. Basch, J. Am. Chem. Soc. 94 (1972) 1451.
[2] M.B. Robin, Higher Excited States of Polyatomic Molecules, 2, Academic Press, New York, 1975.
[3] P. Sherwood, E.A. Seddon, M.F. Guest, M.J. Parkington, T.A. Ryan, K.E. Seddon, J. Chem. Soc. Dalton Trans. 103 (1995) 2359.
[4] G.L. Workman, A.B.F. Duncan, J. Chem. Phys. 52 (1970) 3204.
[5] H. Kato, C. Makochekanwa, M. Hoshino, M. Kimura, H. Cho, T. Kume, A. Yamamoto, H. Tanaka, Chem. Phys. Lett. 425 (2006) 1.
[6] H. Kato, Y. Nunes, D. Duflot, P. Limão-Vieira, and H. Tanaka, J. Phys. Chem. A (2011), submitted for publication, doi:10.1021/jp111063y.
[7] F. Grein, J. Phys. Chem. A 102 (1998) 10869.
[8] I. Hall, I. Cadez, C. Schermann, M. Tronc, Phys. Rev. A 15 (1977) 599.
[9] G.J. Schulz, Phys. Rev. 128 (1962) 178.
[10] (a) A.D. Becke, J. Chem. Phys. 98 (1993) 1372;
(b) C. Lee, W. Yang, R.G. Parr, Phys. Rev. B 37 (1988) 785.
[11] (a) T.H. Dunning Jr., J. Chem. Phys. 90 (1989) 1007;
(b) D.E. Woon, T.H. Dunning Jr., J. Chem. Phys. 98 (1993) 1358.
[12] V.W. Laurie, D.T. Pence, R.H. Jackson, J. Chem. Phys. 37 (1962) 2995.
[13] S.H.D.M. Faria, J.V. da Silva Jr., R.L.A. Haiduke, L.N. Vidal, P.A.M. Vazquez, R.E. Bruns, J. Phys. Chem. A 111 (32) (2007) 7870.
[14] (a) L.S. Cederbaum, J. Phys. B 8 (1975) 290;
(b) J.V. Ortiz, J. Chem. Phys. 89 (1988) 6348.
[15] G.J. Schulz, Rev. Mod. Phys. 45 (1973) 423.
[16] S. Matejcik, T.D. Märk, P. Spanel, D. Smith, T. Jaffke, E. Illenberger, J. Chem. Phys. 102 (1995) 2516.
[17] P. Sulzer, A. Mauracher, S. Denifl, M. Probst, T.D. Märk, P. Scheier, E. Illenberger, Int. J. Mass Spectrom. 266 (2007) 138.
[18] I. Bald, J. Kopyra, E. Illenberger, Angew. Chem. Int. Ed. 45 (2006) 4851.
[19] NIST Chemistry webbook: http://webbook.nist.gov/chemistry.
[20] R. Balog, M. Stano, P. Limão-Vieira, C. König, I. Bald, N.J. Mason, E. Illenberger, J. Chem. Phys. 119 (2003) 10396.